

Document downloaded from:

<http://hdl.handle.net/10251/65710>

This paper must be cited as:

San Emeterio Prieto, J.L.; Rodríguez-Hernández, M.A. (2015). Wavelet Cycle Spinning Denoising of NDE Ultrasonic Signals Using a Random Selection of Shifts. *Journal of Nondestructive Evaluation*. 34(1):1-8. doi:10.1007/s10921-014-0270-8.



The final publication is available at

<http://dx.doi.org/10.1007/s10921-014-0270-8>

Copyright Springer Verlag (Germany)

Additional Information

Wavelet Cycle Spinning Denoising of NDE Ultrasonic Signals Using a Random Selection of Shifts

J.L. San Emeterio¹ and Miguel A. Rodriguez-Hernandez²

(1) Sensors and Ultrasonic Technologies Dept. ITEFI, CSIC, Madrid, Spain,
jluis@ia.cetef.csic.es

(2) ITACA, Universitat Politècnica de València, Spain, marodrig@upvnet.upv.es

Corresponding author:

Miguel A. Rodriguez-Hernandez

ETSI Telecomunicacion

Universitat Politècnica de València

C/ Camino de Vera s/n

46022 Valencia

Spain

e-mail: marodrig@upvnet.upv.es

telephone: (+34) 963879039

fax numbers: (+34) 963879039

Wavelet Cycle Spinning Denoising of NDE Ultrasonic Signals using a Random Selection of Shifts

J.L. San Emeterio¹ and M.A. Rodriguez-Hernandez²

(1) Sensors and Ultrasonic Technologies Dept. ITEFI, CSIC, Madrid, Spain,

jluis@ia.cetef.csic.es

(2) ITACA, Universitat Politècnica de València, Spain, marodrig@upvnet.upv.es

ABSTRACT

Wavelets are a powerful tool for signal and image denoising. Most of the denoising applications in different fields were based on the thresholding of the discrete wavelet transform (DWT) coefficients. Nevertheless, DWT transform is not a time or shift invariant transform and results depend on the selected shift. Improvements on the denoising performance can be obtained using the stationary wavelet transform (SWT) (also called shift-invariant or undecimated wavelet transform). Denoising using SWT has previously shown a robust and usually better performance than denoising using DWT but with a higher computational cost. In this paper, wavelet shrinkage schemes are applied for reducing noise in synthetic and experimental non-destructive evaluation (NDE) ultrasonic A-scans, using DWT and a cycle-spinning implementation of SWT.

A new denoising procedure, which we call Random Partial Cycle Spinning (RPCS), is presented. It is based on a cycle-spinning over a limited number of shifts that are selected in a random way. Wavelet denoising based on DWT, SWT and RPCS have been applied to the same sets of ultrasonic A-scans and their performances in terms of SNR are compared. In all cases three well known threshold selection rules (Universal, Minimax and Sure), with decomposition level dependent selection, have been used. It is shown that the new procedure provides a good robust denoising performance, without the DWT fluctuating performance, and close to SWT but with a much lower computational cost.

Keywords: *wavelets; denoising; ultrasonics; cycle spinning; stationary wavelet transform*

1. Introduction

The detection of small flaws is a difficult problem in ultrasonic non-destructive evaluation (NDE) of composite or highly scattering materials since pulse-echo signals from small defects are frequently masked by noise generated by wave scattering at material microstructure. This grain or structural noise is a type of signal-dependent noise whose frequency spectrum overlaps with the frequency response of the ultrasonic transducer. Usual techniques for white noise reduction, like time averaging or band-pass filtering, are not effective for grain noise reduction. Therefore, specific methods have been proposed, generally based on obtaining spatial or frequency diversity [1-3].

Signal denoising by wavelet shrinkage was introduced by Donoho et al. with applications to white noise reduction [4-6]. The extension of the original method to colored noise problems was performed by using different adaptive thresholds for each frequency band. The values of these new thresholds are related to the energy of the signal at the corresponding wavelet decomposition level. The use of decomposition level dependent thresholds, for reduction of correlated noise using wavelet shrinkage, was introduced in [7].

Noise reduction using wavelets is a well established technique [8]. Most of wavelet denoising procedures rely on the use of the DWT. Unfortunately, DWT is not a time or translation invariant transform and denoising results depend on the selected shift. Improvements on the denoising performance can be obtained using the shift invariant SWT [9-11]. Wavelet denoising using either DWT or SWT is a well established and efficient method for ultrasonic signal denoising. In particular, wavelet techniques have been used for noise reduction and flaw detection in different NDE ultrasonic applications [12-26]. It is considered as a non-parametric method, since any particular model is assumed and therefore any parameter must be estimated.

The main limitation of DWT is that denoising results depend on the selected shift. The SWT denoising procedure includes all the possible shifts implying a high computational cost. An intermediate alternative is proposed in this work using a limited number of shifts, maintaining the quality of SWT denoising method but reducing the computational cost. In the intermediate procedure an important aspect is the selection of shifts. A first option is a fixed selection of shifts, but wavelet denoising is considered a non-parametric method and with this option it is necessary the selection of the shifts for each case and the results are sensitive to the selected shifts. A random selection of shifts maintains the non-parametric nature of the method and the results do not depend in a deterministic way of the selected shifts, also this selection method presents certain variability in repeated executions which could be useful in some applications.

In this work, a new denoising procedure, which we call Random Partial Cycle Spinning (RPCS) is presented and applied to denoise synthetic and experimental ultrasonic A-scans. This

procedure is based on a) a cycle-spinning over a limited number of shifts and b) a random selection of these time shifts. Some preliminary results were previously presented [26]. In this paper, an implementation based on $J+1$ time shifts (being J the maximum DWT decomposition level) is analysed. Wavelet denoising based on DWT, SWT and RPCS have been applied to the same sets of ultrasonic A-scans and their performances measured in terms of signal to noise ratio (SNR) are compared. In all cases three well known threshold selection rules (Universal, Minimax and Sure), with decomposition level dependent selection, have been used.

Several sets of 1000 synthetic ultrasonic A-scans with increasing initial SNR have been generated. In particular, 15 initial sets have been denoised using the different procedures (each one resulting in 9 denoised sets: three procedures and three threshold selection rules). For comparison purposes, the mean and standard deviation of the SNR of different sets have been computed. The coefficients of variation (ratio of standard deviation to mean) of the different denoised sets are also presented as a measure of the denoising performance (a robust denoising procedure should yield a high value of the resulting mean SNR value with a low dispersion).

In addition, ultrasonic A-scans have been acquired from a test block made of austenitic steel and the DWT, SWT, and RPCS procedures have been similarly applied to denoise these experimental traces.

2. Denoising by wavelet thresholding using cycle spinning

DWT is usually computed by means of the Mallat's [27] algorithm. The input at each scale is decomposed into two frequency bands by means of the low-pass and high-pass filters corresponding to the mother wavelet. Then, down-sampling is applied and the low-frequency branch constitutes the input for the next iterative decomposition level. DWT generates the same number of wavelet coefficients than the number of samples of the initial ultrasonic trace. DWT denoising basically consists of three steps: a) a DWT transform of the input data; b) a nonlinear thresholding in the transform domain; c) an inverse wavelet transform.

SWT can be implemented by means of the a'trous [28] algorithm, based on the same Mallat's algorithm but omitting down-sampling of data and up-sampling the filter coefficients at each scale (by inserting zeros). The number of wavelet coefficients after SWT decomposition is $L(J+1)$, being J the maximum decomposition level and L the number of samples in A-scan.

An alternative approach consists in applying the DWT Mallat's algorithm to all circularly-shifted instances of the input signal. The term cycle spinning was introduced by Coifman et al [11]. The basic procedure aims to "average-out" the translation dependence of DWT by means of a)

shifting the input data, b) denoising the shifted data; c) un-shifting the denoised data; and d) average the different results. The maximum number of shifts for a shift invariant implementation is 2^J . In theory the maximum number of shifts should be L , but in practice wavelet coefficient are repeated when the shift is greater than 2^J [29]. The final SWT denoised signal is the linear average of the 2^J DWT denoised stages. Clearly, the use of SWT results in a notable increase of the computational cost.

Denoising using SWT has previously shown a more robust and generally better performance than denoising using DWT. It should be noted that a'trous and cycle spinning implementations of SWT are equivalent but denoising results of these procedures are different because the non-linear thresholding in the transform domain. There are some additional advantages of cycle spinning denoising approach (which we do not explore in this paper) like the possibility of parallel processing or the use of different treatments, alternative to the average, for the final combination of the results obtained for each particular shift.

Denoising with CS averaging over a limited number of consecutive shifts has been previously proposed [11]. In this paper, the evolution of the denoising performance, measured in terms of the SNR as a function of the circular shift number, has been studied using synthetic and experimental ultrasonic A-scans. According to the results, we propose the use of non-consecutive circular shifts. In particular, we propose a random selection of the shifts from a uniform distribution in the interval $[1, 2^J]$. We call this procedure Random Partial Cycle Spinning. In this work, we use $J+1$ random shifts.

The selection of threshold values is a key point in global performance of wavelet denoising. Three threshold selection rules, introduced by Donoho et al [4-6], are used in this work: Universal threshold (VisuShrink), Minimax and Sure threshold (SureShrink). They were initially proposed for white noise reduction and have been widely used. Bearing in mind the characteristics of grain noise, threshold values are determined independently for each decomposition level [7] and each shift. Additional threshold selection techniques have been proposed in literature but in this work, in order to analyze RPCS performance, we make comparisons using only these three well known threshold selection rules. Soft thresholding (wavelet shrinkage) is applied to the wavelet coefficients of the different scales. The remaining processing parameters were fixed in this work as follows: highest decomposition level $J = 7$, zero padding for border treatment in transform evaluation, and Daubechies db6 [30] as mother wavelet.

The performance of different denoising procedures has been measured in terms of SNR defined as:

$$\text{SNR} = \text{peak value in target zone} / \sigma(t) \quad (1)$$

where, target zone is defined as a window around the echo signal to be detected and $\sigma(t)$ is the standard deviation of the whole ultrasonic A-scan.

A second parameter to measure the quality of the denoised traces has been utilised, the coefficient of variation (CV) of the SNR:

$$CV(SNR) = \text{Standard deviation (SNR)} / \text{Mean (SNR)} \quad (2)$$

CV (SNR) is used as an alternative and complementary metric to compare the performance of different procedures in the denoising of a large number of signals. A robust denoising procedure should yield a high value of the resulting mean SNR with a low dispersion and therefore a low value of CV(SNR) indicates a good performance.

3. RPCS denoising of synthetic ultrasonic A-scans

Ultrasonic speckle models are frequently used to generate synthetic registers for evaluating the performance of different algorithms [31-32]. In this work, using a previously developed ultrasonic grain noise generator [13], a set of synthetic ultrasonic grain noise registers $N(t)$ have been generated. The noise generator is based on an approximate grain noise model described in the frequency domain [13]. The noise model accounts for frequency dependent material attenuation and frequency dependent scattering, and includes an accurate model for the transducer pulse-echo response that implies the correlation between the spectrums of ultrasonic pulse and noise. The grain model in the frequency domain can be summarized by following expression:

$$N(f) = \left((N_1(f) f^2) H(f) \right) \exp(-\alpha_0 f^4) + N_2(f) \quad (3)$$

where f is frequency, $H(f)$ is the frequency response of the piezoelectric ultrasonic transducer, $N_1(f)$ represents the scatters distribution of the simulated material and α_0 is factor that controls frequency dependent attenuation. An additional Gaussian white noise $N_2(f)$ is added in order to simulate the effects of the ultrasonic and measurement systems.

Synthetic ultrasonic A-scans have been obtained by inserting a flaw signal (modeled as a back-wall echo $S(t)$ of a 1MHz ultrasonic transducer) at a fixed position of each noise register.

$$T_A(t) = N(t) + A \cdot S(t) \quad (4)$$

where $N(t)$ and $S(t)$ have been normalized in amplitude and therefore the value of parameter A determines the SNR of the initial traces.

1000 noise registers have been generated with 4096 data points, sampling frequency 64 Ms/s, and $\alpha_0 = 1.8 \times 10^{-26}$. From the initial 1000 noise registers, several sets of 1000 ultrasonic A-scans have been generated, each set with a different value of the signal amplitude parameter A of expression (3). The amplitude A of the inserted signal controls the initial SNR mean value of each

set. In particular 15 sets of 1000 A-scans have been generated, varying A from A= 0.6, to A=2, with 0.1 increments and the mean values of the SNR of the obtained sets vary from 3.63 to 6.35.

In the following, some denoising results for a single A-scan are presented firstly while results for the different sets of 1000 synthetic A-scans are analyzed lastly.

Figure 1.a shows the time waveform of an ultrasonic A-scan randomly selected from the set of 1000 A-scans generated with A=1. Superimposed in red is the flaw signal inserted at the central position at approximately 32 microseconds. Figure 1.b shows the frequency spectra of A-scan and signal. This figure illustrates some characteristics of ultrasonic grain noise, with a frequency band that partially overlaps the frequency spectrum of the flaw signal to be detected.

The three denoising procedures analyzed in this paper, DWT, SWT, and RPCS have been applied to denoise the ultrasonic trace of figure 1.a. The values of SNR of the initial and denoised traces are summarized in Table 1. It can be noticed: a) the very bad denoising performance using DWT with Universal threshold selection; b) the good performance in all cases with minimax threshold selection; and c) RPCS obtain results similar to SWT with the three types of threshold selection. As an example, the similarity of resulting time waveforms after SWT and RPCS denoising, using Minimax threshold selection can be appreciated in Figure 2.

Table 1. SNR of initial A-scan and denoised versions using different procedures

| | Universal | Minimax | SURE |
|----------------|-----------|---------|------|
| Initial | 4.19 | 4.19 | 4.19 |
| DWT | 2.82 | 8.05 | 6.46 |
| SWT | 6.32 | 8.51 | 7.94 |
| RPCS | 6.76 | 8.55 | 7.76 |

Figure 3 shows the resulting SNR as a function of circular shift number in the denoising of the same ultrasonic A-scan using an implementation of SWT with 2^J circular shifts of the input signal. It can be appreciated how SNR presents fluctuations with a quasi-periodic behaviour for the three types of threshold selection.

Results of denoising the different sets of 1000 ultrasonic A-scans are presented in the following. At first, the set of 1000 synthetic A-scans generated with A= 1 has been denoised with the different procedures using the same set of processing parameters. The efficiency in noise reduction

has been evaluated in terms of the mean value of the SNR. Results for the different procedures are shown in Table 2. The higher mean values of SNR for the three types of threshold selection correspond to SWT processing, but the results using RPCS with only $J+1$ of the time shifts are very close using much lower computational cost.

Table 2. Mean values of SNR for the initial set of 1000 traces generated with $A=1$ and denoised results using different procedures

| | Universal | Minimax | SURE |
|----------------|-----------|---------|------|
| Initial | 4.47 | 4.47 | 4.47 |
| DWT | 4.68 | 8.03 | 6.44 |
| SWT | 5.84 | 8.35 | 7.07 |
| RPCS | 5.98 | 8.35 | 7.09 |

Lastly, the 15 sets of 1000 synthetic A-scans of 4096 data points were denoised using the different procedures. The mean values of the SNR of the initial and denoised sets are shown in Figures 4 for the different types of threshold selection. It can be appreciated how, as an average, SWT performs nearly always better than DWT denoising. It also should be noted that RPCS nearly replicates the performance of SWT. The use of SURE is better than Universal for low values of initial SNR (SNR_{ini}) while Universal threshold provides better result for high values of SNR_{ini} (this is in accordance with previous results obtained with a lower number of A-scans in the different sets). Finally, it should be highlighted the very good performance of denoising with minimax threshold selection rule.

It should be noted that in the processing of the sets of 1000 A-scans we obtain the mean and the standard deviation of the SNR of each set. We could present additional tables and figures for the standard deviation of each case but we think that this would extend unnecessary the paper. For this reason, to summarize these results, we use the coefficient of variation (CV) of the SNR.

Figure 5 shows the results of the different procedures analyzed in this paper. It can be appreciated how with this metric SWT denoising performs always better than DWT denoising. It can also be noted that RPCS nearly replicates the performance of SWT. The good performance of both Minimax and SURE thresholds, with rhombus and cross symbols respectively, can also be appreciated.

4. RPCS denoising of ultrasonic A-scans composed from experimental registers

Ultrasonic traces were acquired from a test block made of austenitic steel with drilled holes, using an ultrasonic transducer of 1MHz centre frequency and a pulse-echo ultrasonic analyzer. Experimental noise registers were acquired from areas without artificial defects and an ultrasonic pulse-echo response of the transducer was obtained using the back wall echo from a methacrylate block [26]. Registers were obtained with 2500 data samples.

From an experimental noise register, several composed ultrasonic A-scans have been generated by inserting in the central position of the noise register the measured transducer pulse-echo response, which constitutes the flaw signal to be detected. Normalizing in amplitude the noise register and the flaw signal and controlling the amplitude parameter A (as in equation 3), different composed A-scans have been generated with different value of the initial SNR.

Figure 6.a shows the time waveform of the ultrasonic A-scan obtained with $A=0.8$, where superimposed in red is the flaw signal inserted in the central position at approximately 53 microseconds. Figure 6.b shows the frequency spectra of the A-scan and pulse-echo signal. This figure illustrates again some characteristics of experimental ultrasonic grain noise, with a frequency band that overlaps the frequency spectrum of the flaw signal to be detected.

The three denoising procedures analyzed in this paper, DWT, SWT, and RPCS have been applied, similarly to the previous section, to denoise the ultrasonic A-scan of figure 6.a. The values of SNR of the initial and denoised traces are summarized in Table 3. It can be noticed: a) the bad performance in all denoising cases when using Universal threshold selection; b) the good performance in all denoising cases with minimax threshold selection; and c) RPCS obtains a performance similar to SWT with the three types of threshold selection. As an example, the similarity of time waveforms after SWT and RPCS denoising, using Minimax threshold selection can be appreciated in Figure 7.

Table 3. SNR of initial experimental composed A-scans and denoised results using different procedures

| | Universal | Minimax | SURE |
|----------------|-----------|---------|------|
| Initial | 4.33 | 4.33 | 4.33 |
| DWT | 2.53 | 7.29 | 7.09 |
| SWT | 4.26 | 9.01 | 6.64 |
| RPCS | 4.09 | 9.00 | 6.95 |

Figure 8 shows the resulting SNR as a function of shift number in the denoising of the experimental ultrasonic A-scan of figure 6.a, using an implementation of SWT with 2^J circular shifts of the input signal (). Similarly to figure 3, fluctuations and quasi-periodicities are present in SNR. This figure also illustrates how the results of DWT denoising with SURE threshold selection (first point in the figure with shift = 0) are better than the results with SWT and RPCS. The random shifts for RPCS implementation in the processing of these composed traces were selected in shorter interval $[1, 2^{J-2}]$, due to signal length and quasi-periodicities shown in this figure.

Changing the value of the amplitude parameter, from $A=0.6$ to $A=2$ with 0.1 increments, 15 composed experimental ultrasonic A-scans have been obtained, with initial SNR varying from 3.74 to 7.71. These traces have been used for evaluating the influence of the input SNR on the different denoising procedures. As previously done, these A-scans have been denoised combining the three processing algorithm (DWT, SWT and RPCS) with the three thresholds (Universal, Minimax and Sure) resulting in 9 denoised register for each initial trace. Figure 9 shows the SNR of initial and denoised traces as functions of A for the three types of threshold selection. The use of Universal thresholds yields very bad results for the detection of weak signals in all cases. A good performance of RPCS close to SWT, maintaining its quality and robustness, but reducing the computational cost, can be observed in all cases. A good performance in signal denoising for low values of SNR_{ini} can be noted for the different procedures when using Minimax and SURE threshold selection.

5. Discussion

The shift dependence of the denoising performance, measured in terms of the SNR has been studied in this paper using synthetic and experimental ultrasonic A-scans. The SNR of shifted A-scans as a function of shift number (2^J total number of shifts) shows fluctuations with quasi-periodic behaviour. In particular, figures 3 and 8 provide an insight in the performance of cycle spinning procedures: i) they illustrate some quasi-periodicities that are present in the cycle spinning implementation; ii) the SNR after SWT denoising is also displayed in a red line; iii) the fluctuations on SNR explain that in some cases SNR after DWT denoising can be better than SNR after SWT denoising; iv) results of SWT are more robust although at the cost of a higher computational cost. Finally, from this figure it can be easily understood that, in the case of a limited number of shifts, a random selection of shifts is generally better than a consecutive selection of shifts. Circular consecutive shifts (right, left or half left and half right) will tend to maintain DWT performance (either good or bad) while a non-consecutive selection will provide a more robust performance like SWT.

The RPCS denoising procedure implies a random selection of the time shifts. As a consequence there is an intrinsic variability in the denoising performance. We have study this variability using 100 random generations of the time shifts (100 different execution of the RPCS procedure). We have found that the variability is small especially for Minimax and Sure threshold selection which in addition provide a better denoising performance. In consequence, RPCS can be considered as a robust and efficient denoising procedure with a performance close to that of SWT but with a lower computational cost.

The computational cost of DWT algorithm is well established, resulting of order N , being N the number of samples of the A-scan. The computational cost for the present RPCS denoising implementation is approximately $J+1$ times the cost of DWT denoising procedure. The computational cost of a cycle spinning implementation of SWT is initially 2^J times the cost of DWT denoising procedure. Alternatively, RPCS can be implemented with a number of shifts lower than $J+1$ and a selection of these shifts in a shorter interval.

6. Conclusions

A new wavelet shrinkage scheme, based on a quasi translation invariant transform, is presented and applied to noise reduction in synthetic and experimental ultrasonic A-scans. The new denoising procedure, Random Partial Cycle Spinning (RPCS), is based on a cycle-spinning over a limited number of shifts and a random selection of these time shifts. In particular, an implementation based on $J+1$ time shifts (being J the maximum decomposition level) is proposed, but it should be noted that RPCS can be implemented with a lower number of shifts.

Several experiments comparing the new RPCS wavelet shrinkage algorithm with others based on SWT and DWT have been presented. In these experiments three threshold selection rules have been used (Universal, Minimax and Sure) with decomposition level dependent threshold selection in all cases. Evaluations and comparisons presented in this paper provide an insight into the way the translations of the input signal influences the denoising performance.

It is shown that the new procedure maintains a performance close to that of SWT with a much lower computational cost, avoiding the fluctuating results of DWT denoising. The new procedure is effective and provides a good robust performance with only $J+1$ time shifts. CS denoising approach presents additional advantages such as a possible parallel processing as well as alternative methods for the combination of the denoised circular shifted versions. It is a simple robust procedure amenable to real-time implementation.

Acknowledgement: This work was partially supported by Spanish MCI Project DPI2011-22438

References

- [1] Galloway RL, McDermott BA, Thurstone FL (1988) A frequency diversity process for speckle reduction in real-time ultrasonic images. *IEEE Transactions on Ultrasonics, Ferroelectrics and Frequency Control* 35:45-49.
- [2] Newhouse VL, Bilgutay NM, Saniie J, Furgason ES (1982) Flaw-to-grain echo enhancement by Split spectrum processing. *Ultrasonics* 20:59-68.
- [3] Karpur P, Canelones OJ (1992) Split spectrum processing: a new filtering approach for improved signal-to-noise ratio enhancement of ultrasonic signals. *Ultrasonics* 30: 351-357.
- [4] Donoho DL, Johnstone IM (1994) Ideal spatial adaptation by wavelet shrinkage. *Biometrika* 81:425-455.
- [5] Donoho DL, Johnstone IM, Kerkycharian G, Picard D (1995) Wavelet shrinkage: Asymptotia?. *Journal of the Royal Statistical Society Series B* 57:301-369.
- [6] Donoho DL, Johnstone IM (1995) Adapting to unknown smoothness via wavelet shrinkage. *Journal of the American Statistical Association* 90:1200-1224.
- [7] Johnstone IM, Silverman BW (1997) Wavelet threshold estimators for data with correlated noise. *Journal of the Royal Statistical Society* 59:319-351.
- [8] Jansen M (2001) Noise reduction by wavelet thresholding. *Lecture Notes in Statistics* 161 Springer-Verlag. doi:10.1007/978-1-4613-0145-5
- [9] Nason GP, Silverman BW (1995) The stationary wavelet transform and some statistical Applications In: *Wavelets and Statistics, Lecture Notes in Statistics* 103, Springer-Verlag pp 281-299.
- [10] Lang M, Guo H, Odegard JE, Burrus CS (1996) Noise reduction using an Undecimated Discrete Wavelet Transform. *IEEE Signal Proc. Letters* 3:10-12.
- [11] Coifman RR, Donoho DL (1995) Translation-invariant de-noising. In: *Wavelets and Statistics, Lecture Notes in Statistics* 103, Springer-Verlag pp 125-150.
- [12] Abbate A, Koay J, Frankel J, Schroeder SC, Das P (1997) Signal detection and noise suppression using a wavelet transform signal processor: Application to ultrasonic flaw detection. *IEEE Transactions on Ultrasonics, Ferroelectrics and Frequency Control* 44:14-26.
- [13] Lázaro JC, San Emeterio JL, Ramos A, Fernandez JL (2002) Influence of thresholding procedures in ultrasonic grain noise reduction using wavelets. *Ultrasonics* 40:263-267.
- [14] Matz V, Smid R, Starman S, Kreidl M (2009) Signal-to-noise ratio enhancement based on wavelet filtering in ultrasonic testing. *Ultrasonics* 49:752-759.

- [15] Kubinyi M, Kreibich O, Neuzil J, Smid R (2011) EMAT noise suppression using information fusion in stationary wavelet packets. *IEEE Transactions on Ultrasonics, Ferroelectrics and Frequency Control* 58:1027-1036.
- [16] Shi GM, Chen XY, Song XX, Qui F., Ding A.L (2011) Signal matching wavelet for ultrasonic flaw detection in high background noise. *IEEE Transactions on Ultrasonics, Ferroelectrics and Frequency Control* 58:776-787.
- [17] Song SP, Que PW (2006) Wavelet based noise suppression technique and its application to ultrasonic flaw detection. *Ultrasonics* 44:188-193.
- [18] Rodriguez MA, San Emeterio JL, Lázaro JC, Ramos A (2004) Ultrasonic flaw detection in NDE of highly scattering materials using wavelet and Wigner-Ville transform processing. *Ultrasonics* 42:847-851.
- [19] Zhang GM, Zhang SY, Wang YW (2000) Application of adaptive time-frequency decomposition in ultrasonic NDE of highly-scattering materials. *Ultrasonics* 38:961-964.
- [20] Draï R, Khelil M, Benchaala A (2002) Time frequency and wavelet transform applied to selected problems in ultrasonics NDE. *NDT & E International* 35:567-572.
- [21] Pardo E, San Emeterio JL, Rodriguez MA, Ramos A (2006) Noise Reduction in Ultrasonic NDT using Undecimated Wavelet Transforms. *Ultrasonics* 44: e1063-e1067.
- [22] Kechida A, Draï R; Guessoum A (2012) Texture Analysis for Flaw Detection in Ultrasonic Images. *Journal of Nondestructive Evaluation* 31:108-116. doi:10.1007/s10921-011-0126-4
- [23] Rucka M, Wilde K (2013) Experimental Study on Ultrasonic Monitoring of Splitting Failure in Reinforced Concrete. *Journal of Nondestructive Evaluation* 32:372-383. doi: 10.1007/s10921-013-0191-y
- [24] Hosseini SMH, Duzcek S, Gabbert U (2014) Damage Localization in Plates Using Mode Conversion Characteristics of Ultrasonic Guided Waves. *Journal of Nondestructive Evaluation* 33:152-165. doi:10.1007/s10921-013-0211-y
- [25] Mohammed MS, Ki-Seong K (2012) Shift-invariant wavelet packet for signal de-noising in ultrasonic testing. *Insight* 54:366-370.
- [26] San Emeterio JL, Rodriguez-Hernandez MA (2012) Wavelet Denoising of Ultrasonic A-scans by Random Partial Cycle Spinning. In Proc. of the 2012 IEEE International Ultrasonics Symposium pp 455-458.
- [27] Mallat SG (1989) A theory of multiresolution signal decomposition: The wavelet representation. *IEEE Trans. Pattern Anal. Machine Intell.* 11:674-693.
- [28] Shensa MJ (1992) The discrete wavelet transform: wedding the à trous and Mallat algorithms. *IEEE Transactions on Signal Processing* 40:2464-2482. doi: 10.1109/78.157290

- [29] Beylkin G, Coifman R, Rokhlin V (1991) Fast Wavelet Transforms and Numerical Algorithms. *Communications on Pure and Applied Mathematics* 44:141-183.
- [30] Daubechies I (1992) Ten lectures on wavelets. SIAM Philadelphia.
- [31] Romijn RL, Thijssen JM, Vanbeuningen GWJ (1989) Estimation of scatterer size from backscattered ultrasound: A simulation study. *IEEE Transactions on Ultrasonics, Ferroelectrics and Frequency Control* 36:593-606.
- [32] Gustafsson MG, Stepinski T (1997) Studies of split spectrum processing, optimal detection, and maximum likelihood amplitude estimation using a simple clutter model. *Ultrasonics* 35:31-53.

Captions

Figure 1 Ultrasonic A-scan composed from synthetic noise register and pulse modeled as a back-wall echo (a), and frequency spectra of pulse and A-scan (b)

Figure 2 Denoised synthetic A-scans after SWT and RPCS processing using Minimax threshold selection

Figure 3 SNR as a function of shift number in the denoising of A-scan of figure 1 using SWT with 2^J circular shifts. Red dotted line: SNR after SWT denoising.

Figure 4 Mean values of the SNR after denoising of 1000 A-scans in each of the different sets for the different types of threshold selection

Figure 5 Coefficients of variation of the SNR of the different denoised sets of A-scans

Figure 6 Ultrasonic A-scan composed from experimental noise register and transducer back wall pulse echo (a), and frequency spectra of pulse and A-scan (b)

Figure 7 Results of denoising the A-scan of figure 6.a using SWT and RPCS processing with Minimax threshold selection

Figure 8 SNR as a function of shift number in the denoising of A-scan of figure 6 using SWT with 2^J circular shifts. Red dotted line: SNR after SWT denoising.

Figure 9 SNR resulting after different denoising procedures for composed experimental A-scans with increasing values of the initial SNR

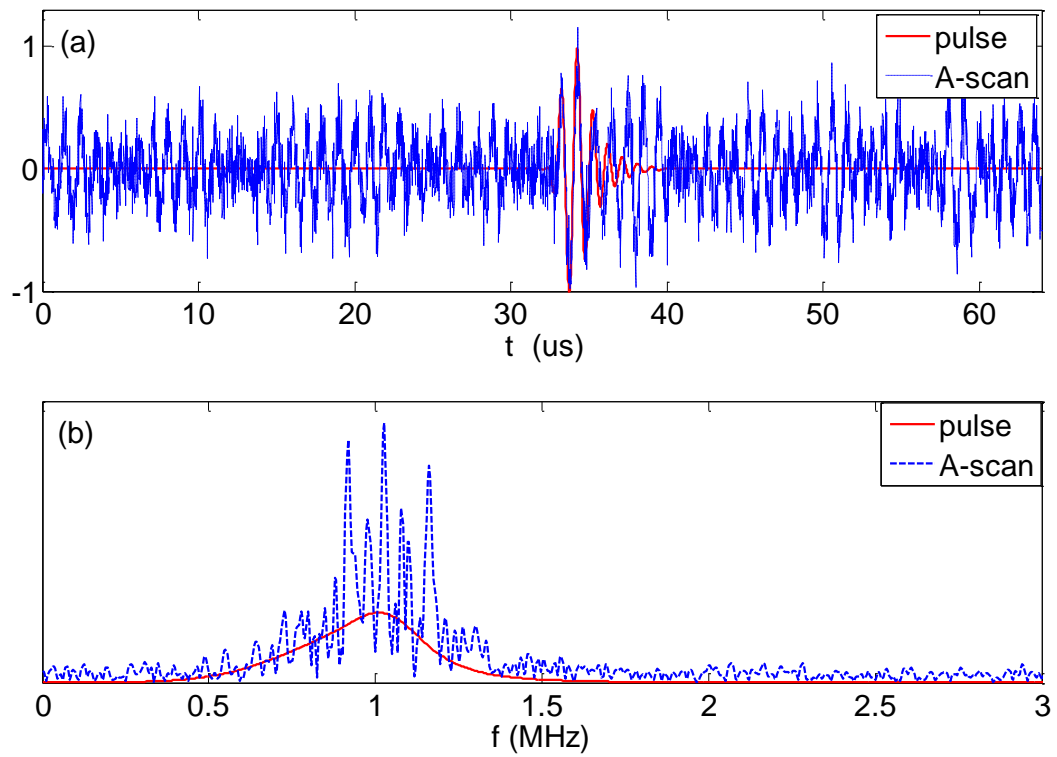


Figure 1 Ultrasonic A-scan composed from synthetic noise register and pulse modeled as a back-wall echo (a), and frequency spectra of pulse and A-scan (b)

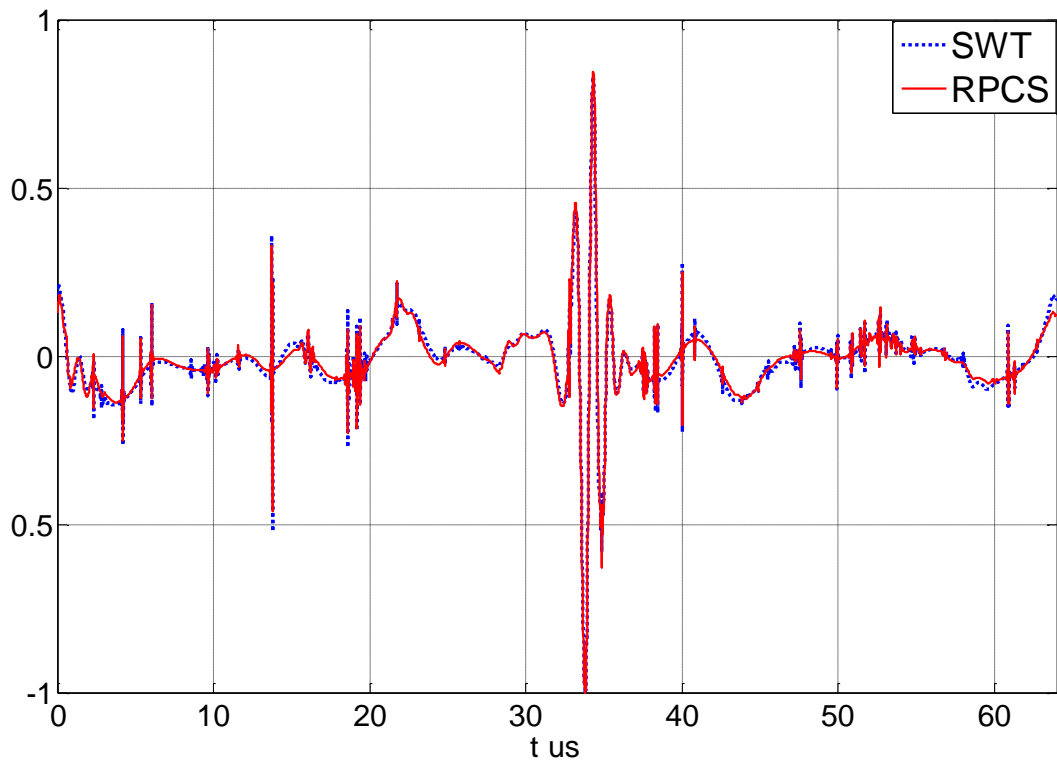


Figure 2 Denoised synthetic A-scans after SWT and RPCS processing using Minimax threshold selection

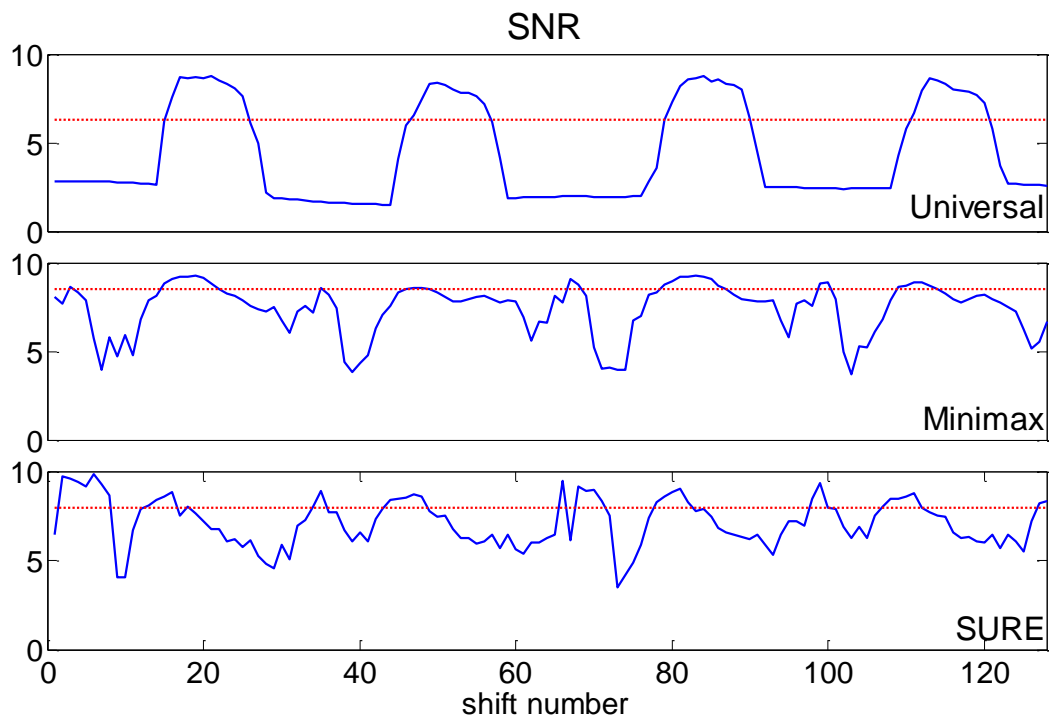


Figure 3 SNR as a function of shift number in the denoising of A-scan of figure 1 using SWT with 2^J circular shifts. Red dotted line: SNR after SWT denoising.

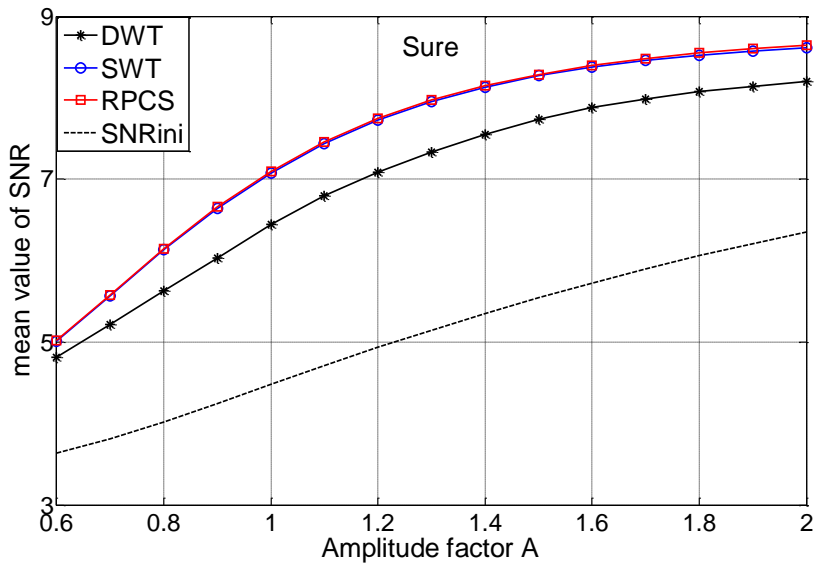
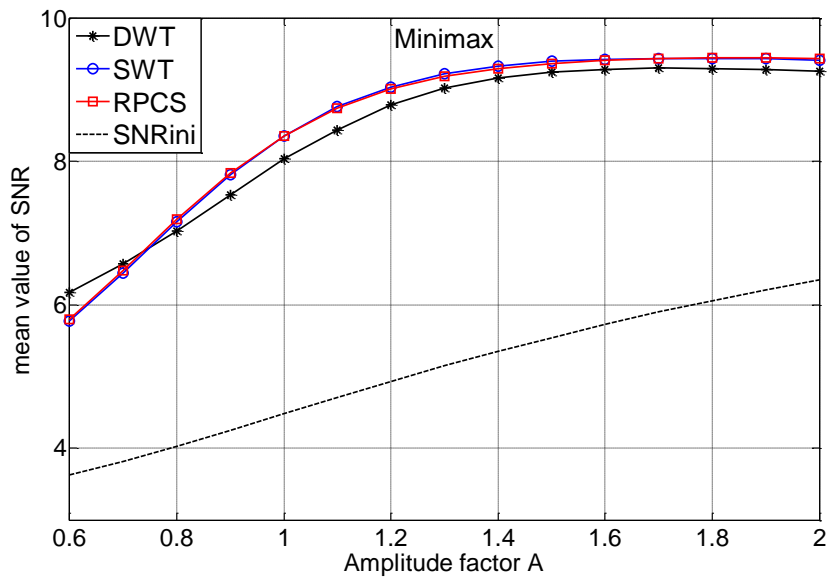
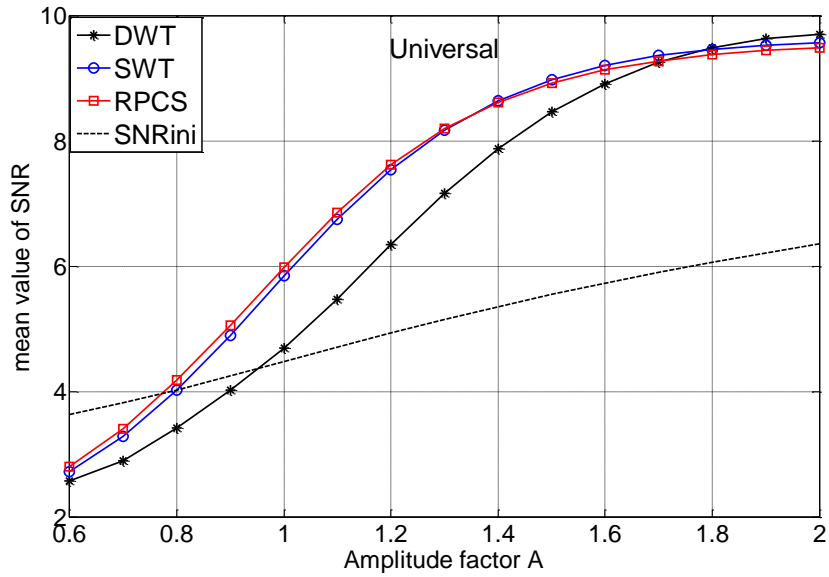


Figure 4 Mean values of the SNR after denoising of 1000 A-scans in each of the different sets for the different types of threshold selection

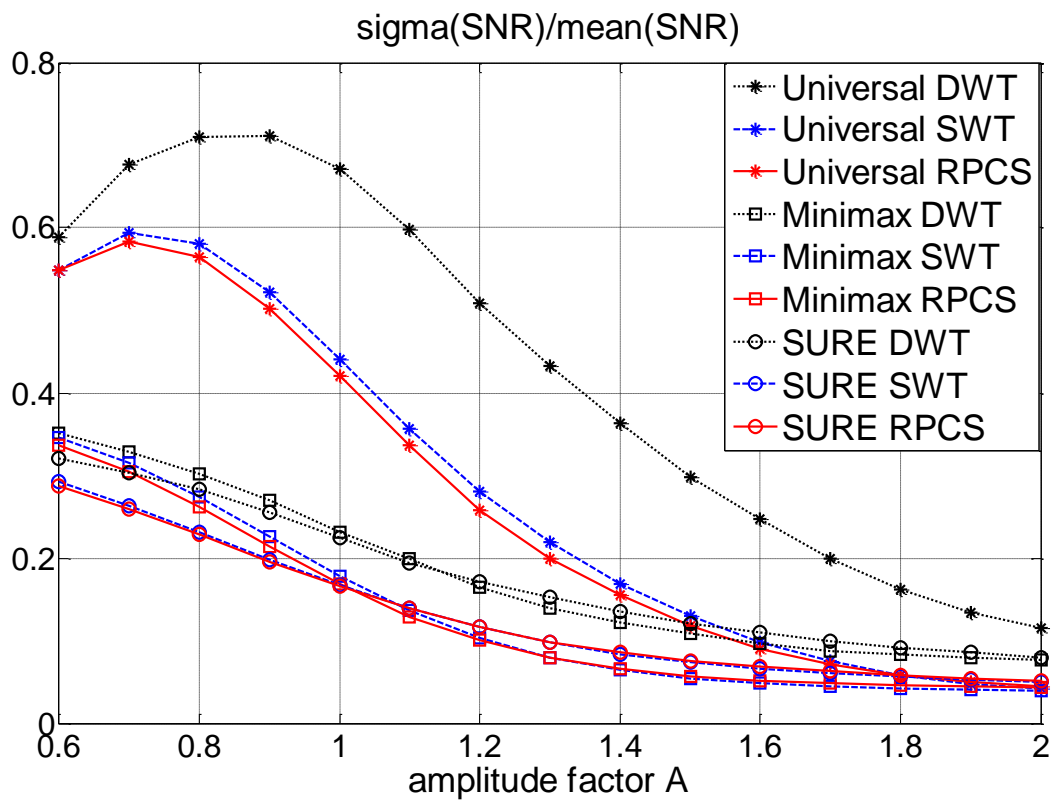


Figure 5 Coefficients of variation of the SNR of the different denoised sets of A-scans

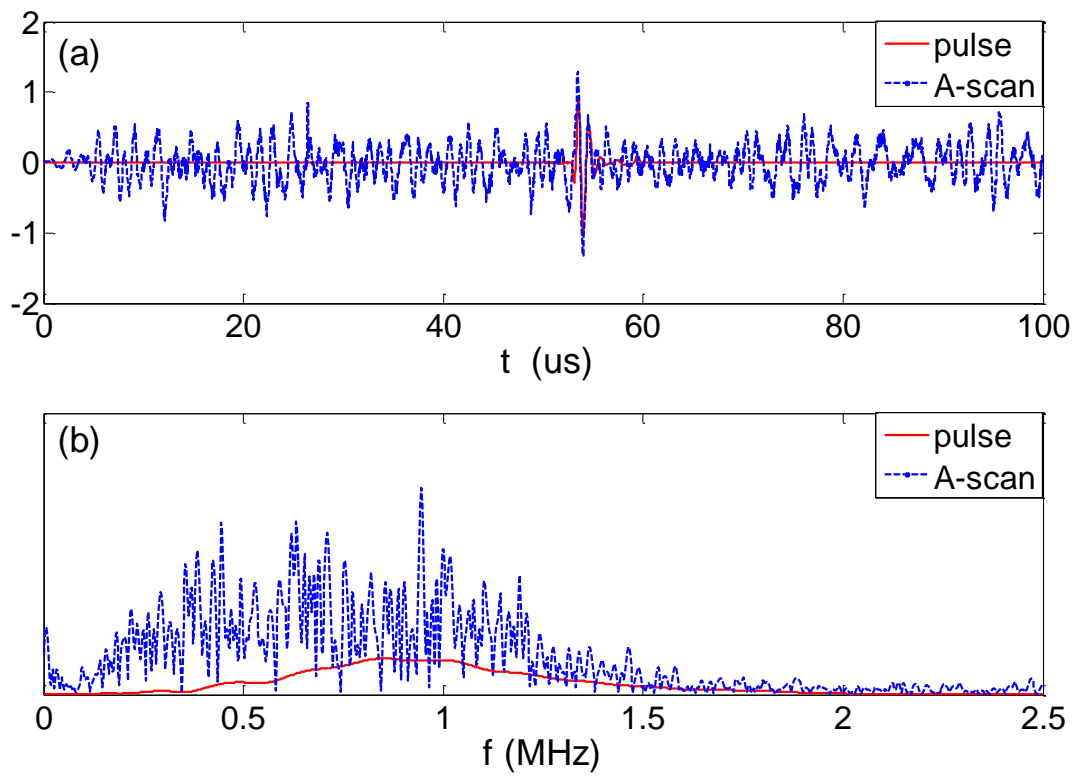


Figure 6 Ultrasonic A-scan composed from experimental noise register and transducer back wall pulse echo (a), and frequency spectra of pulse and A-scan (b)

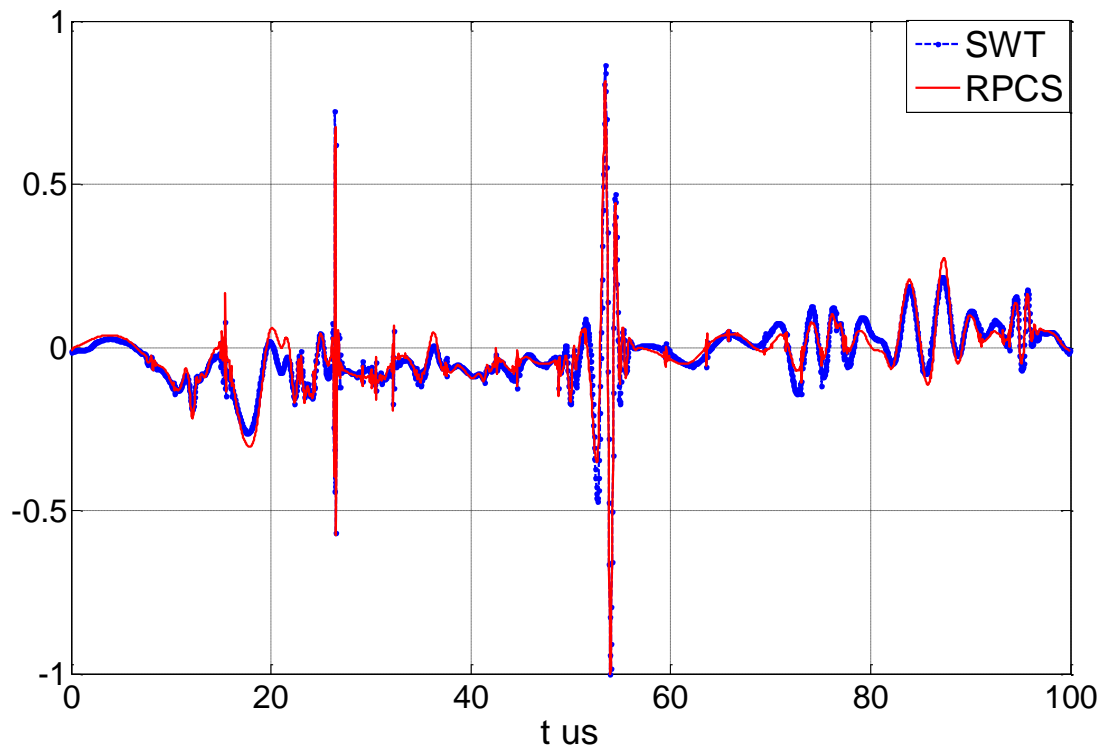


Figure 7 Results of denoising the A-scan of figure 6.a using SWT and RPCS processing with Minimax threshold selection

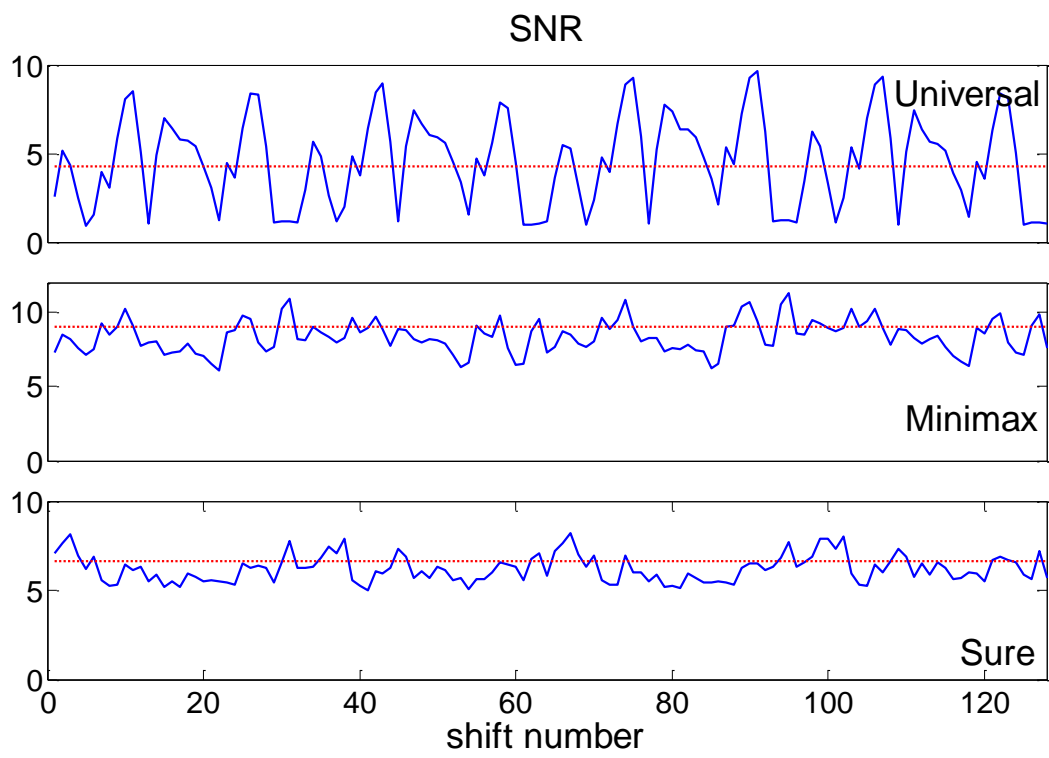


Figure 8 SNR as a function of shift number in the denoising of A-scan of figure 6 using SWT with 2^J circular shifts. Red dotted line: SNR after SWT denoising.

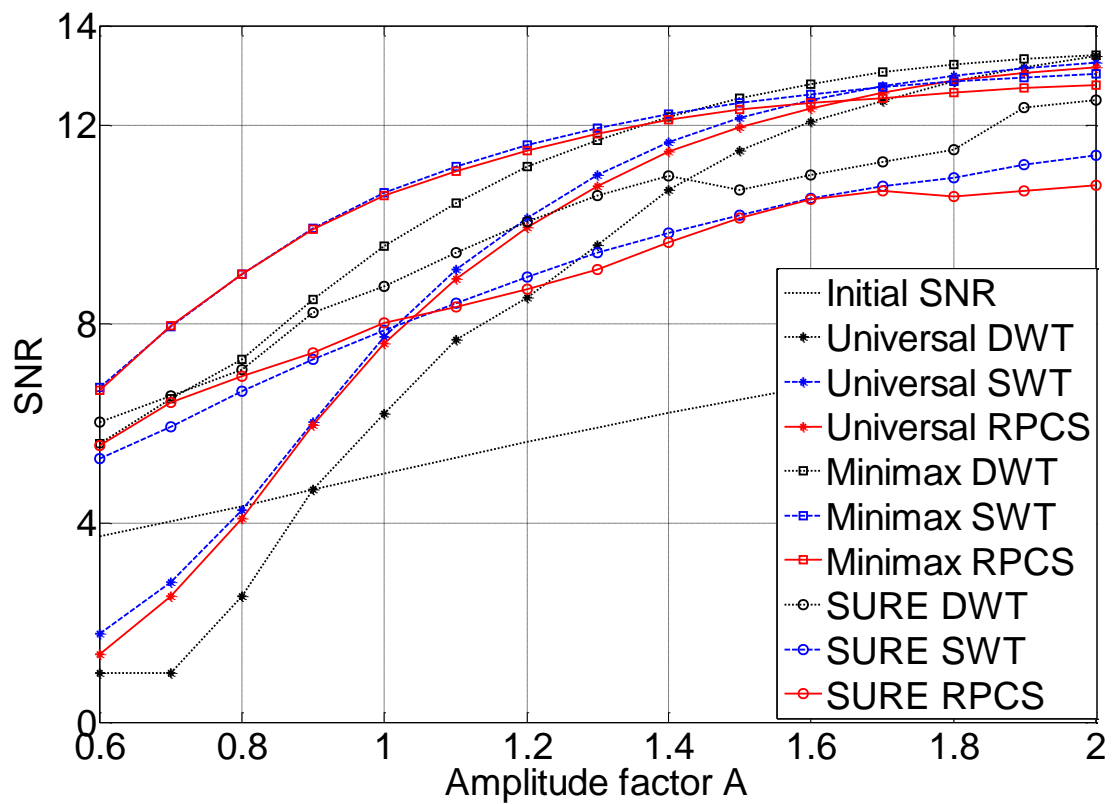


Figure 9 SNR resulting after different denoising procedures for composed experimental A-scans with increasing values of the initial SNR